

# Accepted Manuscript

Texture features for object salience

Kasim Terzić, Sai Krishna, J.M.H. du Buf

PII: S0262-8856(17)30158-0  
DOI: doi:[10.1016/j.imavis.2017.09.007](https://doi.org/10.1016/j.imavis.2017.09.007)  
Reference: IMAVIS 3651

To appear in: *Image and Vision Computing*

Received date: 15 November 2016  
Revised date: 2 July 2017  
Accepted date: 18 September 2017



Please cite this article as: Kasim Terzić, Sai Krishna, J.M.H. du Buf, Texture features for object salience, *Image and Vision Computing* (2017), doi:[10.1016/j.imavis.2017.09.007](https://doi.org/10.1016/j.imavis.2017.09.007)

This is a PDF file of an unedited manuscript that has been accepted for publication. As a service to our customers we are providing this early version of the manuscript. The manuscript will undergo copyediting, typesetting, and review of the resulting proof before it is published in its final form. Please note that during the production process errors may be discovered which could affect the content, and all legal disclaimers that apply to the journal pertain.

# Texture features for object salience

Kasim Terzić<sup>a,c,\*</sup>, Sai Krishna<sup>b</sup>, J.M.H. du Buf<sup>c</sup>

<sup>a</sup>*School of Computer Science, University of St Andrews, Scotland*

<sup>b</sup>*Department of Science and Technology, Centre for Applied Autonomous Sensor Systems, Örebro University, Sweden*

<sup>c</sup>*Department of Electronic Engineering and Computer Science, University of the Algarve, Portugal*

## Abstract

Although texture is important for many vision-related tasks, it is not used in most salience models. As a consequence, there are images where all existing salience algorithms fail. We introduce a novel set of texture features built on top of a fast model of complex cells in striate cortex, i.e., visual area V1. The texture at each position is characterised by the two-dimensional local power spectrum obtained from Gabor filters which are tuned to many scales and orientations. We then apply a parametric model and describe the local spectrum by the combination of two one-dimensional Gaussian approximations: the scale and orientation distributions. The scale distribution indicates whether the texture has a dominant frequency and what frequency it is. Likewise, the orientation distribution attests the degree of anisotropy. We evaluate the features in combination with the state-of-the-art VOCUS2 salience algorithm. We found that using our novel texture features in addition to colour improves AUC by 3.8% on the PASCAL-S dataset when compared to the colour-only baseline, and by 62% on a novel texture-based dataset.

**Keywords:** Texture, Colour, Salience, Attention, Benchmark

## 1. Introduction

The seminal work by Itti, Koch and Niebur [27, 26] included an orientation component from responses of oriented Gabor filters. However, since then, texture has largely been ignored in computational salience models. Most recent work on salience has focused on the pop-out effect primarily caused by colour and intensity, and widely-used benchmarks in this field mostly feature prominent, brightly coloured objects. Colour and intensity are undoubtedly very important cues, but texture can also evoke a pop-out effect; see Fig. 1. Any observer immediately experiences the striking effect in the left image, but most state-of-the-art salience models will fail to identify the salient region. The remarkable success of these models on challenging datasets has unfortunately led to a neglect of texture as an attentional cue.

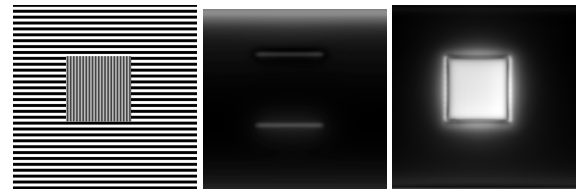


Figure 1: An example of texture salience. The textured region in the left image leads to a strong pop-out effect, despite it having the same average colour and intensity as the surrounding region. Blob detection based on colour therefore fails in this case (middle image). However, blob detection based on texture features, as described in this paper, detects the salient blob (right image).

In this paper, we revisit the Itti and Koch model and examine which types of features are well-suited to detecting salient regions on the basis of texture. We then propose a simple set of features on top of complex cells. We combine these features with the recent state-of-the-art VOCUS2 algorithm, which evolved from the Itti and Koch framework, in order to demonstrate the effectiveness of our approach. We evaluate our approach on a set of standard datasets, and on a novel dataset which specifically addresses texture.

We see this work as a first step towards a texture-based salience mechanism based on a fast model of cor-

\*Corresponding author at: School of Computer Science, University of St Andrews, Scotland

Email addresses: kt54@st-andrews.ac.uk (Kasim Terzić), sai.krishna@oru.se (Sai Krishna), dubuf@ualg.pt (J.M.H. du Buf)

URL: kt54.host.cs.st-andrews.ac.uk (Kasim Terzić), mpi.aass.oru.se/people/sai-krishna/ (Sai Krishna), w3.ualg.pt/~dubuf/ (J.M.H. du Buf)

tical cells in V1 [54]. To the best of our knowledge, this is the first model of its kind, which can provide a baseline for further work in this area. We do not expect that a purely texture-based approach will ever outperform colour-based approaches. Rather, we are convinced that an additional salience channel can improve existing algorithms in situations where object and background colours are similar.

## 2. Related Work

Visual salience has become one of the central topics in computer vision over the past few decades, and considerably longer in the field of human and biological vision. In order to deal with the inherent complexity of the visual world, biological systems have evolved a way to prioritise information by identifying objects, or parts, which stand out from the rest, and which are likely to characterise the essence of the surrounding scene. The concept of Bayesian surprise has been explored to model this process [25]. Psychophysical experiments have shown that texture is perceived in a pre-attentive fashion [48]. Pre-attentive means bottom-up and data-driven, which is also referred to as covert attention, in contrast to overt, consciously directed attention.

In their influential work, Laurent Itti, Christof Koch and Ernst Niebur [27, 26] introduced a filtering approach to covert attention. Their model, which inspired countless others, extracts salience by a combination of centre-surround DoG filters. They applied these filters to feature maps which consist of colour channels and the responses of oriented Gabor filters, thus mimicking early biological vision. Their model was designed for explaining sequential saccadic eye movements, from the most conspicuous image point to other points with decreasing order of conspicuity and inhibition of return. The recent algorithm VOCUS2 by Frintrop et al. has extended the same principle to detecting larger salient regions instead of points [14], demonstrating the continued usefulness of the concept. The original Itti and Koch model has been extended numerous times, for example by weighting the different feature maps after identifying useful features [24] and by exploring the role of salience in overt attention [46]. In addition, eye fixation maps have been combined with traditional segmentation methods in order to model the segmentation of salient regions [35]. The idea of contrasting the centre of a region against its surround has also been applied using different similarity measures. Bruce and Tsotsos used information content of the two regions [6] for their AIM model, while Klein and Frintrop used the KL di-

vergence of feature statistics [30] and later multivariate probability distributions [31].

Much research in recent years has moved towards detecting entire salient objects in scenes. For testing the methods, there exist several high-profile benchmarks of natural images where the task is to segregate a prominent object. Most of the current approaches try to segment an entire object, and regions can be modelled according to their colour and luminance [1], contrast [9, 8] or dissimilarity [13]. Another approach is to learn a correct foreground object segmentation from a set of training images [38]. This object-based salience can be very important for providing top-down feedback for scene understanding in artificial intelligence [51, 43] and cognitive robotics [53, 32]. Yet other methods try to represent the scene in terms of visual perception [17], graph-based visual salience [21], and object-based salience features [20]. Additionally, salience has also been modelled as a discriminant process [16] and as a regression problem [28]. Multi-scale processing has been shown to improve salience on small-scale, high-contrast patterns [59].

Despite the vast variety of developed methods, almost all are based on colour and intensity. These feature channels are very convenient: an object with largely constant colour which differs from the colour of its background will generate a strong response from an appropriately-sized centre-surround filter. However, the prevalence of colour-based features is also partly due to the way that modern benchmarks have been designed: most images feature brightly-coloured objects that are particularly suited to being identified by colour. Unfortunately, this benchmarking aspect has contributed to the neglect of other important feature channels. The result is that a completely trivial example as shown in Fig. 1 defeats nearly every available salience algorithm. This example creates a pop-out effect solely on the basis of texture, not colour nor intensity, and only very few salience methods explicitly employ spatial frequency or texture. The original Itti and Koch model included responses of oriented Gabor filters as one of the feature channels, so at least local orientation could play a role. However, this feature was found not to contribute strongly to the final results, and in recent variations of the Itti and Koch model this channel is ignored altogether [14]. Achanta et al. [2] used bandpass filtering to obtain uniform regions with sharp boundaries, but their features were still based on colour. Texture models have typically been used for texture segmentation, and are often built on top of Gabor filter responses, followed by further processing such as spatial averages of local neural responses [39]. Alternatively, a bank of

matched filters for specific textures can be used [33], but performance becomes limited by the representativeness of the chosen filters. Wavelets have also been used to successfully classify different textures [4]. Typically, texture segmentation is based on some kind of feature gradient (or feature contrast), and the maxima represent texture boundaries. Although texture models (and especially Gabor-based texture models) have been extensively benchmarked [18] and successfully used for texture segmentation [44] and classification [4], comparatively few authors have explored their use for salience and attention models.

The earliest work on texture-based salience was probably by Sayeda-Mahmood [48]. The algorithm produces four binary maps from the image, and constructs a number of features, including the total number of holes in a region, the area occupied by holes in a white region, and the shape and distribution of the holes. A heuristic algorithm then combines these into a salience score. The features are complex to compute because they involve region growing, counting and computing convex hulls, and they were only tested on artificial images in a segmentation context. Building on the Itti and Koch model, Li's method [37] employed responses of V1 cells directly to detect pop-out effects in simple textures consisting of oriented textons. This work has been extended to multi-spectral features and a large number of textons [56], although it was only tested on a novel multi-spectral dataset. In [7], texture features are used to detect edges and combined with an object model to fill the rest of the salient object. Kalinke et al. [29] used co-occurrence matrices in order to extract texture-based features for creating hypotheses in an intelligent vehicle scenario. Powerful texture models for video [10, 58] are often difficult to use within the centre-surround filtering context, but they can be used within a discriminative framework [15]. More recently, the eye fixation model of Momtaz and Daliri uses human fixations to train a salience model using features like orientation and spatial frequency [41]. However, most of the above approaches are either difficult to apply within a centre-surround filtering context, or they do not aim to be general enough for salient region detection in natural images.

There are several approaches which build salience maps from the frequency spectrum of the image. The method of Hou and Zhang is based on the global Fourier transform [23]. They subtract the average log-spectrum of many images from the log-spectrum of a specific image. This produces a residual spectrum. When this spectrum is transformed back to the spatial domain, it indicates salient regions which potentially correspond

to objects. Guo et al. [19] built on this concept, but argued that the phase, not the amplitude, of the spectrum is key to finding salient regions. They extended this concept to the Quaternion Fourier Transform which can represent intensity, colour and motion of each pixel. An more recent take on quaternion-based salience was proposed by Schauerte and Stiefelhausen [49], whose method achieved state-of-the-art results on predicting human eye fixations. These methods are not biologically plausible, nor are they based explicitly on texture, but our experiments show that they are more effective at texture salience than colour-based methods.

We are not aware of any recent work on salience which attempts to explicitly model texture and test model parameters on large-scale salience datasets. While there is a wealth of research on texture analysis and segmentation, methods are often difficult to use in a salience setting. In the rest of this paper we present a new and more biological interpretation of the local Gabor filter responses, extending our earlier work [52]. We describe the local texture using a parametric model of the local power spectrum. The parameters of this model represent new features, which are then processed using centre-surround DoG filters.

### 3. Methods

Salient parts of an image are often defined as regions which differ strongly from their surround, which are therefore conspicuous and appear to "pop-out." They can be detected by applying centre-surround filters to a stack of images, where each image represents a certain feature. In general terms, we can define a feature vector  $\mathbf{F}$  consisting of  $N$  independent feature dimensions at each pixel position in the image:

$$\mathbf{F} = [F_1, \dots, F_N] \quad \mathbf{F} \in \mathcal{R}^N. \quad (1)$$

Typically, salience models use colour channels to represent  $\mathbf{F}$ , for example  $\mathbf{F} = [L, a^*, b^*]$ . Here the components represent a pixel's colour in CIELAB space.

The input image can then be represented by a stack of real-valued images, each image in the stack being a different feature dimension at each pixel location:

$$\mathbf{S}(\mathbf{x}) = [I_1(\mathbf{x}), \dots, I_N(\mathbf{x})], \quad (2)$$

where  $\mathbf{x}$  is a vector representing the usually two-dimensional pixel position.

This representation is useful for detecting salient objects defined by intensity or colour. Large areas with nearly constant colour are described by very similar feature vectors, so neighbouring pixels in a colour patch

will have similar values. Thus, salient regions will generate strong responses if filtered by appropriately-sized centre-surround filters. However, as shown in Fig. 1, if the salient region is not defined by colour, intensity or contrast, this approach will fail. If the region is primarily defined by a difference in texture, one must include texture parameters. In general, colour-only or texture-only approaches are prone to failure because there will always exist images in which a salient region is characterised by the other property, and the compromise is to use feature vectors which consist of both colour and texture parameters.

### 3.1. Properties of texture features

We propose that texture features suitable for salience detection should have the following three properties: constancy, similarity and Euclidean geometry. Although it is conceivable that additional properties could be beneficial, we are here primarily interested in features which fit seamlessly into the centre-surround filtering framework.

*Euclidean geometry.* The feature vector  $\mathbf{F}$  should contain real-valued elements, as defined in Eq. 1. The individual images  $I_n$  from the image stack  $\mathbf{S}$  can then be filtered independently by a bank of centre-surround filters. The filtering operation is naturally performed in the space of real values, since it only requires multiplication, addition and negative values. Colour coding in CIELAB space fulfils this criterion.

*Constancy.* A large, homogeneous texture should result in a constant feature representation. This way, large textured regions will produce no internal response when filtered by a centre-surround filter. At the same time, a small, differently textured region embedded within a large region should generate a strong response. CIELAB colour features exhibit constancy in case of homogeneously coloured regions, but they may not be constant within a homogeneous texture. For example, when one or more colour components are modulated periodically, so will be the corresponding features. In such a case success depends on the colour components of the small region and its surrounding region, and their periodicities must be much smaller than the centre Gaussian of the DoG kernel.

*Similarity.* Visually similar textures should be represented by similar feature vectors. Visually dissimilar textures should produce very different vectors. Here, too, CIELAB features as used in most salience models are similar for similar colours, but have no relation to

texture unless texture is defined by colour modulation and the above observations with respect to constancy are considered.

It is clear that colour channels (like the  $La^*b^*$  components of CIELAB space) possess the above properties. Below, our goal is to find texture-based features with the same properties, such that they can be used in conjunction with a salience algorithm based on colour channels, in particular an algorithm which employs centre-surround DoG filtering.

### 3.2. Local power spectrum

Our texture features are based on the local image spectrum at each pixel location. In this section, we explain how a local spectrum can be obtained from Gabor filter responses.

Simple cells in area V1 of the visual cortex are often modelled by oriented Gabor filters. The phases of the filters are commonly restricted to obtain odd-symmetric (sine) and even-symmetric (cosine) components. Responses of these odd and even cells can be conveniently represented in quadrature, where the even component represents the real part, and the odd component represents the imaginary part of a complex filter:

$$G_{\lambda,\theta}(x,y) = \exp\left(-\frac{\tilde{x}^2 + \gamma\tilde{y}^2}{2\sigma^2}\right) \exp\left(i\frac{2\pi\tilde{x}}{\lambda}\right), \quad (3)$$

where rotation is defined by

$$\tilde{x} = x \cos \theta + y \sin \theta \quad (4)$$

$$\tilde{y} = y \cos \theta - x \sin \theta, \quad (5)$$

$\lambda$  is the wavelength of the sinusoidal part (in pixels), and  $\sigma$  is the standard deviation of the Gaussian envelope, which controls the receptive field size (also in pixels). Parameter  $\theta$  denotes the orientation of a rotated 2D Gabor filter.

There is a wide range of possible parameter choices, and it is known that V1 cells come in many phases, orientations and receptive field sizes. This leads to a large number of filtering operations, but efficient algorithms exist which work in real time. We rely on the recent implementation from [55], and adopt their default parameters:  $\sigma/\lambda = 0.56$ ,  $\gamma = 0.5$ , and  $\theta$  assumes 8 values equally spaced on  $[0, \pi)$ .  $\lambda$  assumes 9 values, spaced half an octave apart.

Responses of simple cells are obtained by convolving an image  $I$  with the complex Gabor filters,

$$S_{\lambda,\theta}(x,y) = I(x,y) * G_{\lambda,\theta}(x,y). \quad (6)$$

Odd simple cells respond maximally at step stimuli, while even simple cells respond to bars and lines. Complex cells in the visual cortex respond to both, and they are less sensitive to location. One common way to model complex cells is by using the moduli of simple cell responses [22]:

$$C_{\lambda,\theta}(x, y) = |S_{\lambda,\theta}(x, y)|. \quad (7)$$

The advantage of this representation, as opposed to e.g. the HMAX pooling model, is that each complex cell at a given pixel location encodes one part of the local power spectrum. Fig. 2 illustrates this concept: the local power spectrum can be seen as a 2D function over orientation and frequency (scale). Each texture possesses a specific local power spectrum, or “signature.”

The use of many Gabor filters at multiple orientations and scales means that our current algorithm for extracting texture features incurs a penalty of half a second per image. However, our code is not very optimised at the moment and the filtering operation can be more than 10 times faster on a GPU [55].

### 3.3. Spectral texture features

The local power spectrum (Fig. 2) tells us several important things about the texture. The horizontal axis represents the orientations of the complex cells. Vertical stripes in the power spectrum mean that complex cells tuned to a particular orientation respond strongly, and that the texture has a corresponding orientation component. Since the eight filter orientations are evenly spaced on  $[0, \pi)$ , filters with  $\theta = 0$  and  $\theta = (7/8)\pi$  cover neighbouring orientations. Therefore, the local power spectrum should be imagined as being cylindrical or cyclic over orientation. The vertical axis represents the frequency or scale of the complex cells, and it can tell us about the coarseness or fineness of the texture or of its components. In principle, the entire power spectrum can be used as feature vector, but it consists of  $8 \times 9 = 72$  values at each pixel location. Apart from the fact that the use of 72 feature images is prohibitive, the question is whether we really need all the precise information. Since our goal is to have few features which can indicate that an object differs from its surrounding, we aim at a more compact model.

We observed that for many textures the local power spectrum resembles a 2D Gaussian function [11]. This means that often the power is clustered around one orientation and one scale. This is partly due to a property of the V1 model we use: each complex cell is tuned to a specific orientation and scale, but cells tuned to similar orientations and scales also respond, be it less, effectively yielding a smooth power spectrum. Although

a 2D Gaussian spectrum is a crude approximation for many real-world textures, for example those with two dominant orientations, it still contains important information which can be useful for distinguishing different textures. In our model, the 2D Gaussian spectrum is represented by the mean scale and orientation,  $\mu_s$  and  $\mu_o$ , and the spreads around these, the standard deviations  $\sigma_s$  and  $\sigma_o$ . Fig. 2 illustrates the parameters.

These four parameters have a very intuitive interpretation.  $\mu_s$  and  $\mu_o$  indicate the dominant scale and orientation, and can thus differentiate between coarse and fine textures, and textures with different orientations.  $\sigma_o$  represents a texture’s isotropy: a small value means that a texture is anisotropic with one pronounced orientation, whereas a large value indicates the presence of multiple orientations. Similarly,  $\sigma_s$  indicates the mixture of scales. A small value means one, well-defined scale, while a large value means that the texture contains both coarse and fine elements.

The 2D array holding the local power spectrum is processed using a very quick algorithm. Since the spectrum is typically noisy, it is first smoothed by a lowpass  $3 \times 3$  block filter. This filter is applied to the “cylindrical” array which is cyclic in the orientation dimension. Then, two projections are computed by summing the array into two 1D arrays: the scale array  $S_i$  and the (also cyclic) orientation array  $O_i$ . In each of these arrays, the local maximum is found, yielding  $\mu_s$  and  $\mu_o$ . Here, the local maximum is used as a rough approximation of the mean of the fitted Gaussian which is faster and did not negatively affect performance in our tests. Finally, the standard deviations  $\sigma_s$  and  $\sigma_o$  around  $\mu_s$  and  $\mu_o$  are determined, taking again into account the periodicity of  $O_i$ . Although true 1D or 2D curve fitting leads to more accurate values, in practice we did not find significant differences in the salience results. We must not forget that the four parameters are still to be processed by big DoG filters, i.e., big lowpass filters before the subtraction. Therefore, in our evaluation we use the simpler approach. Figure 3 illustrates the features in case of a real input image from Achanta et al. [1].

### 3.4. Salience extraction

Once an image is processed by our spectral algorithm, it is represented by a stack of four feature images similar to an RGB, HSV or CIELAB colour stack. As discussed earlier, the features extracted by our algorithm also behave in a similar way as colour features, so they can be used as direct input to a standard salience algorithm. Our work aims at finding texture features which are compatible with the centre-surround filtering framework for blob detection.

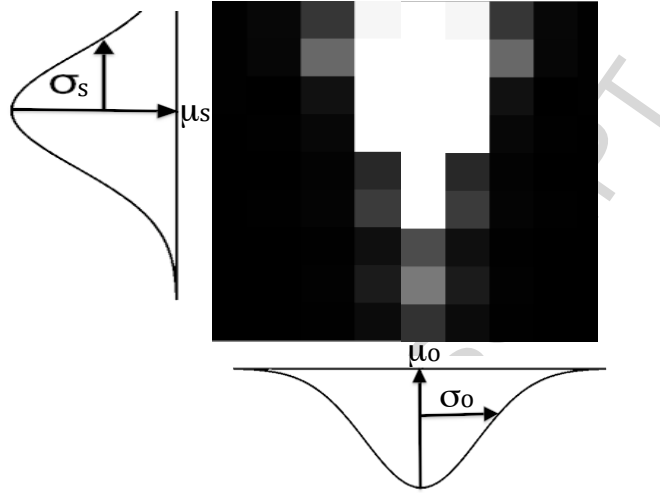


Figure 2: Our texture model. A local power spectrum is a 2D matrix with the dimensions representing orientation (horizontal axis) and frequency (vertical). This spectrum often resembles a 2D Gaussian function. We therefore fit two 1D Gaussians to the 1D marginal arrays to obtain the means and standard deviations of orientation and frequency, which we use as features.

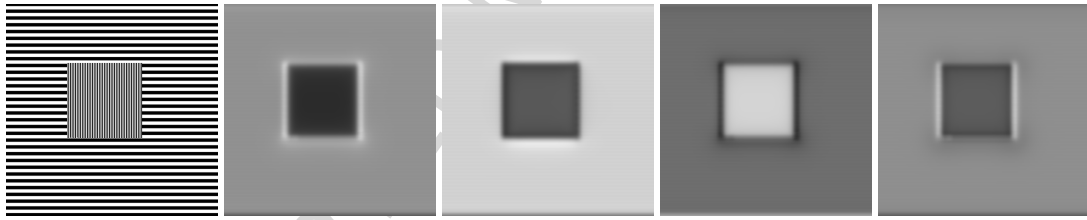


Figure 3: Example of texture features extracted from a synthetic image. Blob detection on these feature maps is used to produce a salience map. From left: input image,  $\mu_o$ ,  $\sigma_o$ ,  $\mu_f$ ,  $\sigma_f$ .

In order to evaluate the effects of our features in a fair way, we decided to use an off-the-shelf state-of-the-art algorithm which implements a variation of the Itti and Koch model. The VOCUS2 algorithm [14] has recently shown strong performance across a wide range of salience benchmarks, and we therefore employ it in our evaluation. Our main motivation was to perform a fair comparison between standard colour-based features and our new texture-based ones on a set of difficult and texture-dominated images.

In our tests, we used three versions of this salience detector. The first is the default version, using three colour-based channels as input: intensity, red/green, and blue/yellow. Each of these feature channels is processed by a set of centre-surround filters to produce a conspicuity map for each channel. These conspicuity maps are then summed to create the salience map [14]. The second version uses our four feature maps (mean and standard deviation of orientation and scale at each pixel) instead of the colour/intensity maps. The result is a

salience map derived purely from our texture model. The final, complete version uses a combination of all available features: three colour-based, plus four texture based, for a total of seven input feature maps.

#### 4. Evaluation

We evaluated our features on three standard datasets: MSRA-1000 [1], PASCAL-S [36], and ECSSD [50]. Additionally, we tested on a novel texture dataset which was designed to test how sensitive existing salience algorithms are to texture. We report the precision-recall curve and the Area Under Curve (AUC).

Our method used our texture features as input to the standard VOCUS2 algorithm, with and without colour channels. We compared against standard VOCUS2 algorithm [14], the two frequency-based algorithms by Guo et al. [19] and Hou et al. [23], information-theoretic approach AIM [6], the Codi method [31], Quaternion saliency [49], and the state-of-the-art deep learning

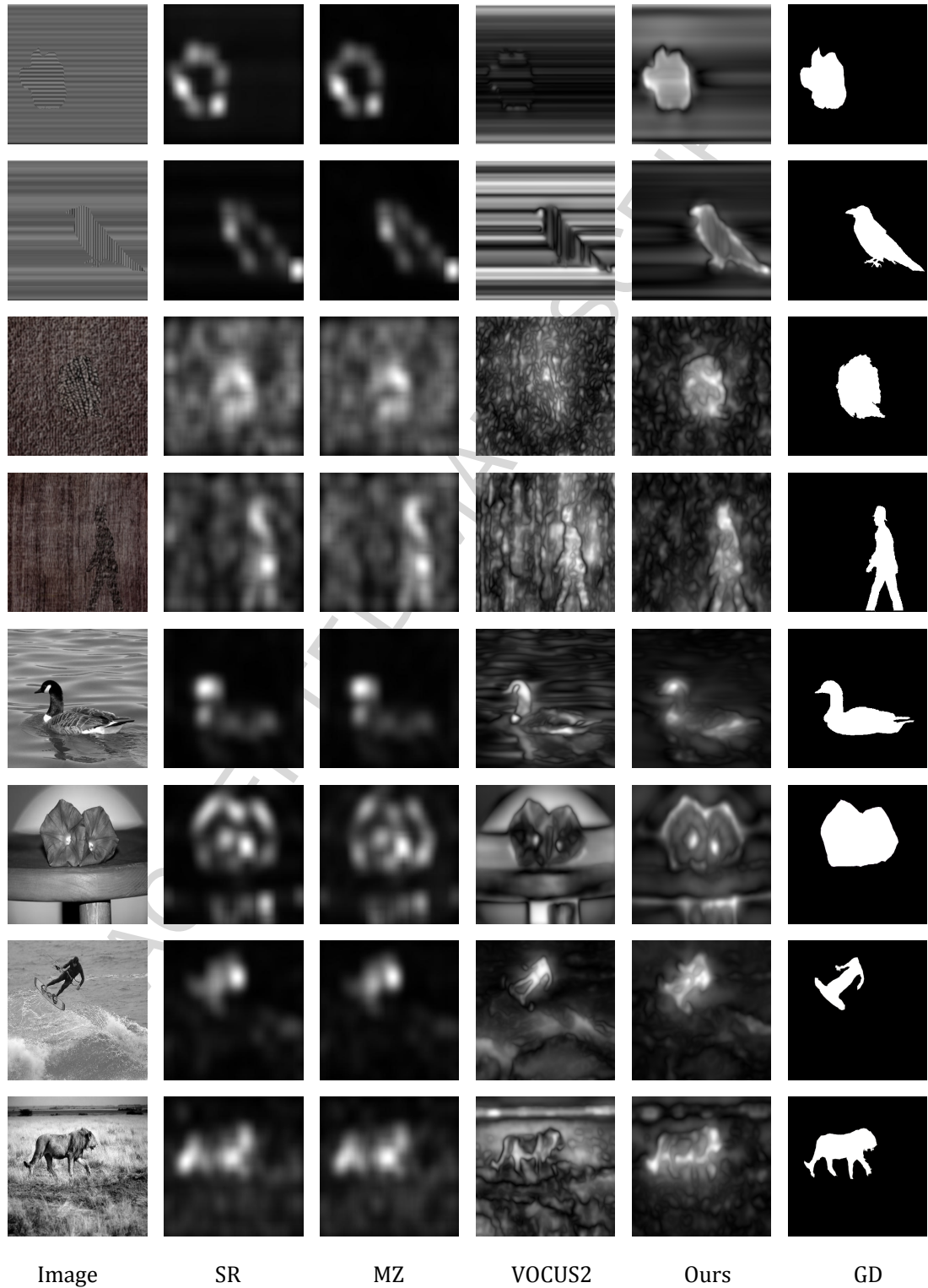


Figure 4: Visual comparison of results on the new texture salience dataset. The input images are shown on the left, the ground truth annotations on the right. The other columns, from left to right, show the results of the spectral residual (SR) method [23], of the phase spectrum (MZ) method [19], of the standard VOCUS2 method based on colour [14], and our new texture features used together with VOCUS2. All images are before thresholding them with different threshold values for computing precision-recall curves.



method SalGAN [45]. The latter was included to establish the current state of the art on natural datasets but we stress that our primary goal was to measure the influence of texture features and evaluate their usefulness in a salience context.

#### 4.1. Natural image datasets

We tested on three standard natural image datasets: MSRA-1000, PASCAL-S, and ECSSD. The datasets consist of images accompanied by ground-truth masks indicating salient objects. Performance is reported as a precision-recall curve calculated on a pixel-wise basis.

Figure 5 shows the results on the MSRA-1000 dataset by Achanta et al. Texture-based methods all performed poorly on this dataset. Standard colour-based VOCUS2 method outperformed our complete method which combines colour and texture, but both of them outperformed the deep learning method SalGAN.

We then tested on two more recent and more challenging datasets: PASCAL-S and ECSSD (Fig. 6). As expected, the deep-learning method did very well here, followed by our complete method which combined texture and colour. On both of these datasets, the addition of texture features boosted the result compared to the standard, colour-only VOCUS2: by 3.2% on ECSSD and by 3.8% on PASCAL-S. This confirms our intuition that texture features improve performance on natural images. Codi performed slightly worse than standard VOCUS2, and all texture-only methods performed much worse. This was expected because texture is a weaker attention cue than colour. However, it shows that texture alone carries important information about salience, and that integrating texture features is beneficial.

#### 4.2. Texture-based dataset

We then tested the algorithms on a novel dataset. This dataset also consists of 1000 images, but the images were created such that texture is the main driver of attention. It consists of three subsets: a synthetic dataset, a mixed dataset, and a modified natural dataset.

The synthetic dataset consists of 300 artificial images filled with artificial textures. The textures exhibit systematic variations in scale, orientation and isotropy. This subset tests the basic behaviour of the algorithms in a controlled manner. For example, see the top two rows of Fig.4.

The second, mixed dataset uses combinations of natural textures and consists of 400 images. Ground-truth annotations were taken from various images of the Achanta dataset, and the foreground and background

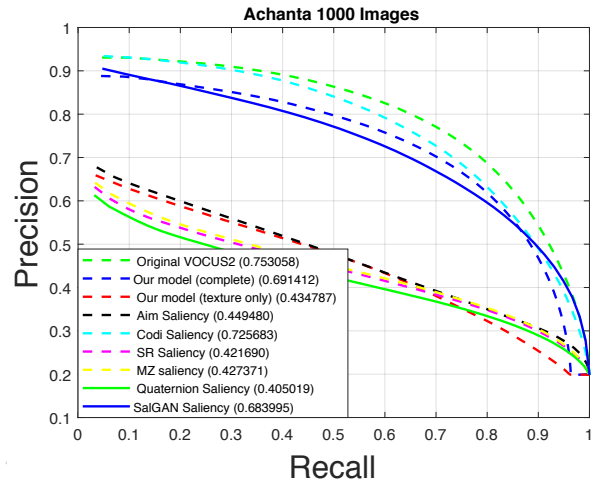


Figure 5: Evaluation on the standard MSRA-1000 salience dataset [1]. Our texture features combined with the VOCUS2 algorithm outperform the frequency-based methods SR [23] and MZ [19], but do worse than the original VOCUS2 algorithm [14] which is based on colour and intensity. Texture was not found to be a strong cue on this dataset, with texture-based methods doing poorly. The use of texture features failed to improve performance of VOCUS2 on this dataset.

were filled with different natural textures selected from [5]. This subset tests the ability of the features to represent complex, real-world textures.

The third subset consists of 300 modified images from the Achanta set. The images were converted to greyscale in order to remove colour. This subset tests the strength of the features in scenarios where intensity and colour are unreliable cues.

The results on this dataset are shown in Fig. 7. As expected, colour-based methods VOCUS2 and Codi performed worst in the absence of colour, but the frequency-based approaches performed much better than they did on the natural dataset. This indicates that the frequency spectrum of the image is much better at capturing texture information than colour channels. Our texture-only method does very well on this dataset. When combining our texture features with colour, the result is even better, largely because intensity is a useful cue in the modified subset. It is interesting to note that the deep-learning method performs well on this dataset, which shows that it managed to learn some texture-based features. However, it is clearly outperformed by our two texture-based methods. This shows that even simple explicit texture features are powerful cues. On this dataset, the use of texture features together with colour features boosts the AUC score of VOCUS2 by 62%.

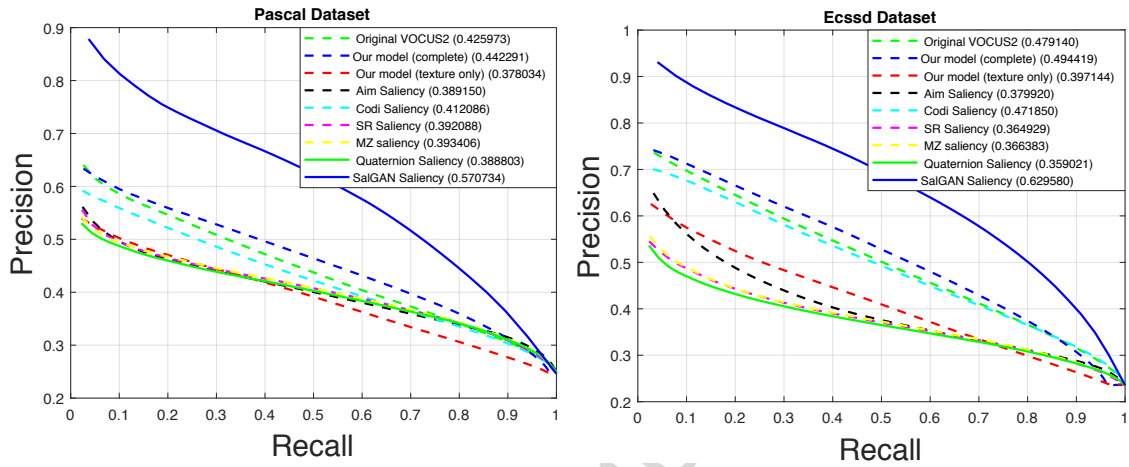


Figure 6: Evaluation on the PASCAL-S (left) and ECSSD (right) datasets. The deep learning method does best, but it can be clearly seen that the use of texture features improves the performance of the VOCUS2 algorithm. All texture-based methods perform similarly on the PASCAL-S dataset, but our texture-only algorithm clearly outperforms other texture-based methods on the ECSSD dataset.

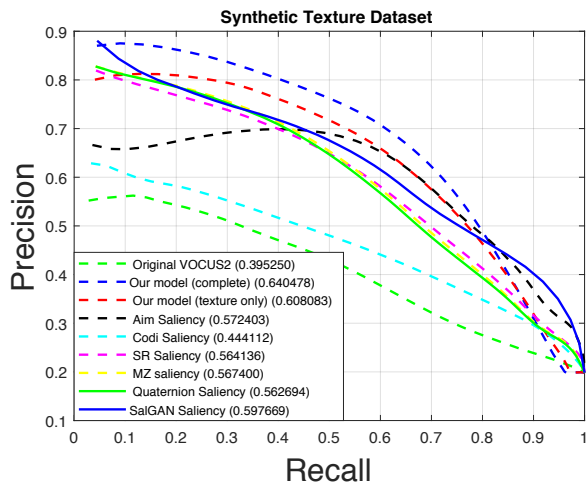


Figure 7: Comparison on the new texture saliency dataset. Here our texture-based features outperform all other tested methods, including VOCUS2 [14], spectral residual (SR) [23], and phase spectrum (MZ) [19]. It can be seen that colour and intensity perform very poorly on this dataset, unlike the proposed texture features. Deep saliency (SalGAN) performs well, but not as well as our texture-based approach.

## 5. Discussion

Our experiments on standard datasets show that texture is clearly not the main driver of saliency. This is not surprising, and was to be expected from the success of colour-based methods on natural images. The results, however, strongly suggest that adding texture features to colour-based features increases performance and manages to significantly outperform existing spectrum-based methods. These conclusions are still

premature, because the texture model is extremely simple with only four parameters.

Texture obviously plays a role in human vision, and there are many toy examples where colour-based saliency methods fail, so an important part of the puzzle is still missing from our saliency models. Our new dataset was built specifically to test the ability of algorithms to detect salient objects primarily defined by texture, and the results clearly show that texture models are needed for this. On this new dataset, colour-based VOCUS2 did very poorly, although it is consistently among the top-performing algorithms on a wide range of standard saliency datasets [14]. The spectral methods of Hou et al. [23] and Guo et al. [19] significantly outperformed it, although they are not competitive at all on the original natural dataset of Achanta et al. As expected, our features excel in case of texture-driven saliency. Interestingly, the state-of-the-art method based on deep learning performed well on this task, but was still outperformed by our simple texture model.

### 5.1. Biological plausibility

Striate cortex, or visual area V1, can be seen as a unique buffer which is available for any computations which require high resolution details and spatial precision. Higher, extrastriate areas V2, V4 etc. form a hierarchy with feedback to V1. Without this feedback, vision is not possible. Low-level computations in V1 cannot be completed before high-level computations in V2 etc. are begun, and V1 is computing different types of information during the 40-350 ms post-stimulus time period. Edges and other local features are computed

first, involving only V1, but 3D shape, figure-ground and object reconstruction are done later, and these require feedback from V4/MT and even inferior-temporal (IT) cortex [34].

Vision is based on the interplay of all parts. V1 may be a high-resolution buffer which holds a precise reconstruction of an object and its position, it has no understanding of what it holds. In contrast, IT cortex knows what the object is but not where it is. Therefore, vision requires both V1 and IT cortex, and it follows that figure-ground segregation and object recognition are intertwined. All available information can be combined for segregation: optical flow and stereo disparity normally apply to entire objects, but colour and texture may be problematic because objects can have differently coloured or textured parts.

Segregation and recognition are also related to attention. Early work on Focus-of-Attention (FoA) was based on the idea that some complexity maps, for example salience maps based on colour contrast, provided peaks for modelling saccadic eye movements with inhibition of return to already “visited” peaks (see below). Taking into account that the fusion of colour and disparity information often suffices to obtain the contour of an entire object which can then be employed for a first object categorisation [40], in this paper we did not address saccadic eye movements but exogenous attention to entire objects for object segregation. Instead of employing a filling-in process by neural diffusion or Ullman’s “colouring,” see e.g. [34], a process reminiscent of boundary-filling in computer graphics, segregation is done by building a Gaussian tree such that DoG (Difference-of-Gaussians) filter kernels can be applied. The idea is that the tree can be built in the V1-up hierarchy with increasing kernel size and concurrent loss of spatial localisation, after which feedback down to V1 serves to restore precision. In computer vision, the state-of-the-art VOCUS2 colour salience algorithm already employs blob detection by DoG kernels [14]. Therefore, by using the VOCUS2 algorithm we could focus on texture and easily experiment with colour and texture information.

Figure-ground segregation as outlined above still lacks a process which guides the up and down information streams and maintains attention until up-down convergence has been achieved and all communications between the levels are muted. There is increasing evidence that all cortical areas are connected to the thalamus, that the thalamus is not only a passive relay station (first-order visual thalamus is also called LGN, lateral geniculate nucleus, which receives input from the retinae and forwards this to V1), but that the thalamus must

be seen as an active, volatile blackboard which holds the latest ideas synthesised from multiple cortical sources. The surface layer of the thalamus, the reticular layer or RE thalamus, has a special role: to gate information and to sustain cortical attention. Building on earlier FoA work by Francis Crick and Anne Treisman’s “search-light” metaphor, also taking into account the massive projection from V1 back down to LGN, David Mumford [42] speculated that if the thalamus is the gateway to the cortex, then RE thalamus, “smack in the middle of the pathway,” is the guardian of the pathway. Hence, if V1 is a high-resolution buffer and LGN an internal but also high-resolution sketchpad, with higher areas V2 etc. and higher-order thalamic areas forming concurrent hierarchies holding more complex representations with less localisation at the higher levels, then RE thalamus, which is the only layer known to have connections between thalamic areas, can provide the substrate for the guidance process: to sustain attention to specific objects as information continually and concurrently moves up and down.

## 5.2. Relation to computational models

In computer vision, texture analysis and segmentation are among the most explored but yet unsolved problems. One of the main reasons is that textures can assume all combinations of scales (periodicities) and orientations. They can be stochastic or structured, isotropic or anisotropic. The intra-class variations of materials like stone, wood, glass, fabric and water are enormous and their classification still is a huge challenge [47]. Another reason is that often homogeneously textured regions are assumed and tested, the regions of test images being filled with synthetic textures or real ones from for example the Brodatz collection [5]. In computer vision all research effort has resulted in countless models that can be applied to different texture classes. In biological vision (mammal, primate) this diverse development has not happened, probably because the neural functionality to choose from is rather limited. The most notable exception is offered by simple and complex cells in V1, simple cells often being modelled by Gabor filters with phases in quadrature. These cells and the Gabor model have led to the widespread application of wavelets to texture in computer vision [3]. Apart from these cells, there are hypercomplex cells, also called end-stopped cells because they respond strongly to vertices formed by edge crossings and to blobs, and bar and grating cells. The latter are nonlinear, because a bar cell responds to an isolated bar but not at all to the individual bars in a periodic grating, whereas a grating cell only responds to periodic bars. Indeed, it

has been shown that an advanced model of grating cells can be used to detect periodic textures with only one orientation, but also that multiple cells tuned to different orientations can be used to detect gratings with different symmetries, i.e., rectangular and hexagonal textures [12].

The question is what mechanisms does our visual system deploy for dealing with all types of textures in our everyday tasks. It is well-known that spatial orientation and frequency play an important role in visual attention [57], but less is known about existence of more complex texture models. When developing a texture-based salience model we therefore gave economy a decisive role: the simplest model with only very few parameters on top of existing circuitry, the complex cells. The rationale is that we do not need to model all types of textures; rather, we often need only one parameter which can distinguish an object from its background.

Texture processing in human vision is complex and not yet well understood. It is believed that texture even plays a role in early processing, like segmentation and attention as evidenced by the pop-out effect (Fig. 1). Our features are based directly on complex cells in V1, with relatively simple post-processing. Therefore, the simplicity and good performance of our model might hint at similar early texture coding strategies in biological systems [34].

The behaviour of V1 cells is quite well understood, and we used a well-established model. The interpretation of the responses as a local power spectrum is a bit more difficult to argue, since it essentially is an engineering model which was explored for different texture processing strategies and models [11]. We do not suggest that the visual cortex “intends” to calculate a local power spectrum. However, our features can be extracted from responses of complex cells by very simple additions, multiplications and max operations. It is this simplicity which suggests that it could be a plausible model for early texture processing. In addition, texture features can be easily combined with colour features, and both require simple blob detection, for example by DoG filter kernels in a Gaussian tree. It becomes more complicated when motion and stereo disparity must be integrated, because these are processed in higher areas with feedback to area V1. Motion and disparity are primary cues for object segregation because object recognition is not yet required. These cues could actually steer blob detection for texture and colour, (1) with feedback to V1 in order to obtain precise object contours, and (2) in the entire hierarchy from V1 to IT cortex such that IT cortex knows what it is but not where it is, and V1 has a precise picture of it with absolutely no clue as to what

it is [34].

## 6. Conclusions

In this paper we presented a novel set of features for texture-based salience. To the best of our knowledge, this is the first time that texture features were shown to be a useful salience cue, and the first time that a texture-based model is evaluated on a large dataset. Two other algorithms used (global) spectral image characteristics for salience [23, 19]. In contrast, our proposed features model texture explicitly, the model is about the simplest one that one can conceive, the four parameters have very intuitive interpretations in terms of isotropy and scale.

We also introduced a new dataset which is specifically designed to test the ability of a salience detector to deal with texture. It comprises a mix of synthetic images, of artificial images with natural textures, and of natural images without colour information. The evaluation shows that the addition of texture features to a centre-surround method yields improved results both on natural images and on a novel texture dataset, suggesting that texture can be useful for salience. We believe that this dataset will also be useful to other researchers in this field.

*Acknowledgements.* This work was supported by the EU under the FP-7 grant ICT-2009.2.1-270247 *Neural-Dynamics* and by the FCT under the grants LarSYS UID/EEA/50009/2013 and SparseCoding EXPL/EEI-SII/1982/2013.

## References

- [1] R. Achanta, F. J. Estrada, P. Wils, and S. Süsstrunk. Salient region detection and segmentation. In *ICVS*, pages 66–75, 2008.
- [2] R. Achanta, S. S. Hemami, F. J. Estrada, and S. Süsstrunk. Frequency-tuned salient region detection. In *CVPR*, pages 1597–1604, 2009.
- [3] A. Ahmadvand and M. R. Daliri. Invariant texture classification using a spatial filter bank in multi-resolution analysis. *Image Vision Comput.*, 45:1–10, 2016.
- [4] A. Ahmadvand and M. R. Daliri. Rotation invariant texture classification using extended wavelet channel combining and ll channel filter bank. *Knowledge-Based Systems*, 97:75–88, 2016.
- [5] P. Brodatz. *Textures: a photographic album for artists and designers*. Dover Publications, Inc., New York, 1966.
- [6] N. D. B. Bruce and J. K. Tsotsos. Saliency, attention, and visual search: An information theoretic approach. *Journal of Vision*, 9(5), March 2009.
- [7] H-Y Chen and J-J Leou. A new visual attention model using texture and object features. In *IEEE CIT Workshops*, pages 374–378, July 2008.
- [8] M.-M. Cheng, N. J. Mitra, X. Huang, P. H. S. Torr, and S.-M. Hu. Global contrast based salient region detection. *IEEE T-PAMI*, 37(3):569–582, March 2015.

- [9] M-M Cheng, G-X Zhang, N. J. Mitra, X. Huang, and S-M Hu. Global contrast based salient region detection. In *CVPR*, pages 409–416, 2011.
- [10] G. Doretto, A. Chiuso, Y. N. Wu, and S. Soatto. Dynamic textures. *Int. J. Comput. Vis.*, 51, 2003.
- [11] J. M. H. du Buf. Abstract processes in texture discrimination. *Spatial Vision*, 6:221–242, 1992.
- [12] J. M. H. du Buf. Improved grating and bar cell models in cortical area v1 and texture coding. *Image Vision Comput.*, 25:873–882, 2007.
- [13] L. Duan, C. Wu, J. Miao, L. Qing, and Y. Fu. Visual saliency detection by spatially weighted dissimilarity. In *CVPR*, pages 473–480, 2011.
- [14] S. Frintrop, T. Werner, and G. Martin-Garcia. Traditional saliency reloaded: A good old model in new shape. In *CVPR*, 2015.
- [15] D. Gao, V. Mahadevan, and N. Vasconcelos. The discriminant center-surround hypothesis for bottom-up saliency. In *NIPS*, pages 497–504, 2008.
- [16] D. Gao and N. Vasconcelos. Bottom-up saliency is a discriminant process. In *ICCV*, pages 1–6, 2007.
- [17] S. Goferman, L. Zelnik-Manor, and A. Tal. Context-aware saliency detection. In *CVPR*, pages 2376–2383, 2010.
- [18] S. E. Grigorescu, N. Petkov, and P. Kruizinga. Comparison of texture features based on gabor filters. *IEEE Transactions on Image Processing*, 11(10):1160–1167, October 2002.
- [19] C. Guo, Q. Ma, and L. Zhang. Spatio-temporal saliency detection using phase spectrum of quaternion fourier transform. In *CVPR*, 2008.
- [20] J. Han, K. N. Ngan, M.J. Li, and H.J. Zhang. Unsupervised extraction of visual attention objects in color images. *IEEE Trans. Circuits Syst. Video Techn.*, 16(1):141–145, 2006.
- [21] J. Harel, C. Koch, and P. Perona. Graph-based visual saliency. In *NIPS*, pages 545–552, 2006.
- [22] F. Heitger, L. Rosenthaler, R. von der Heydt, E. Peterhans, and O. Kuebler. Simulation of neural contour mechanisms: from simple to end-stopped cells. *Vision Res.*, 32(5):963–981, 1992.
- [23] X. Hou and L. Zhang. Saliency detection: A spectral residual approach. In *CVPR*, 2007.
- [24] Y. Hu, X. Xie, W.-Y. Ma, L.-T. Chia, and D. Rajan. Salient region detection using weighted feature maps based on the human visual attention model. In *PCM*, pages 993–1000, 2004.
- [25] L. Itti and P. Baldi. Bayesian surprise attracts human attention. In *NIPS*, pages 547–554, 2005.
- [26] L. Itti and C. Koch. A saliency-based search mechanism for overt and covert shifts of visual attention. *Vision Research*, 40(10-12):1489–1506, May 2000.
- [27] L. Itti, C. Koch, and E. Niebur. A model of saliency-based visual attention for rapid scene analysis. *IEEE Trans. Pattern Anal. Mach. Intell.*, 20(11):1254–1259, 1998.
- [28] H. Jiang, J. Wang, Z. Yuan, Y. Wu, and N. Zheng. Salient object detection: a discriminative regional feature integration approach. In *CVPR*, 2013.
- [29] T. Kalinke, C. Tzomakas, and W. von Seelen. A texture-based object detection and an adaptive model-based classification. In *Proc. IEEE Intelligent Vehicles Symposium*, volume 98, pages 341–346, 1998.
- [30] D. A. Klein and S. Frintrop. Center-surround divergence of feature statistics for salient object detection. In *ICCV*, 2011.
- [31] D. A. Klein, G. M. García, and S. Frintrop. A computational model for saliency detection based on probability distributions. In *European Conference on Visual Perception (ECPV)*, Alghero, September 2012.
- [32] A. Kreutzmann, K. Terzić, and B. Neumann. Context-aware classification for incremental scene interpretation. In *Workshop on Use of Context in Vision Processing*, Boston, November 2009.
- [33] M. S. Landy and J. R. Bergen. Texture segregation and orientation gradient. *Vision Research*, 31(4):679–691, 1991.
- [34] T. S. Lee, D. Mumford, R. Romero, and V. A. F. Lamme. The role of the primary visual cortex in higher level vision. *Vision Res.*, 38:2429–2454, 1998.
- [35] Y. Li, X. Hou, C. Koch, J. M. Rehag, and A. L. Yuille. The secrets of salient object segmentation. In *CVPR*, pages 280–287, 2014.
- [36] Y. Li, X. Hou, C. Koch, J. M. Rehag, and A. L. Yuille. The secrets of salient object segmentation. In *CVPR*, pages 280–287, Washington, DC, USA, 2014.
- [37] Z. Li. A saliency map in primary visual cortex. 6(1):9–16, January 2002.
- [38] T. Liu, J. Sun, N. Zheng, X. Tang, and H.-Y. Shum. Learning to detect a salient object. In *CVPR*, 2007.
- [39] J. Malik and P. Perona. Preattentive texture discrimination with early vision mechanisms. *J. Opt. Soc. Am. A*, 7(5):923–932, May 1990.
- [40] J. A. Martins, J. M. F. Rodrigues, and J. M. H. du Buf. Proto-object categorisation and local gist vision using low-level spatial features. *BioSystems*, 135:35–49, 2015.
- [41] H. Z. Momtaz and M. R. Daliri. Predicting the eye fixation locations in the gray scale images in the visual scenes with different semantic contents. *Cogn Neurodyn*, 10:31–47, 2016.
- [42] D. Mumford. On the computational architecture of the neo-cortex. i. the role of the thalamo-cortical loop. *Biol. Cybern.*, 65:135–145, 1991.
- [43] B. Neumann and K. Terzić. Context-based probabilistic scene interpretation. In *IFIP AI*, pages 155–164, Sep 2010.
- [44] T. Ojala and Pietikinen M. Unsupervised texture segmentation using feature distributions. *Pattern Recognition*, 32(3):477–486, March 1999.
- [45] J. Pan, E. Sayrol, X. Giro i Nieto, C. C. Ferrer, J. Torres, K. McGuinness, and N. O’Connor. Salgan: Visual saliency prediction with adversarial networks. In *CVPR Scene Understanding Workshop (SUNw)*, July 2017. Accepted.
- [46] D. Parkhurst, K. Law, and E. Niebur. Modeling the role of salience in the allocation of overt visual attention. *Vision Res.*, 42(1):107–123, Jan 2002.
- [47] X. Qi, L. Shen, G. Zhao, Q. Li, and M. Pietikäinen. Globally rotation invariant multi-scale co-occurrence local binary pattern. *Image Vision Comput.*, 43:16–26, 2015.
- [48] T.F. Sayeda-Mahmood. Detecting perceptually salient texture regions in images. *Computer Vision and Image Understanding*, 76(1):93–108, October 1999.
- [49] B. Schauerte and R. Stiefelhagen. Quaternion-based spectral saliency detection for eye fixation prediction. In *ECCV*, pages 116–129, 2012.
- [50] J. Shi, Q. Yan, L. Xu, and J. Jia. Hierarchical image saliency detection on extended cssd. *IEEE TPAMI*, 38(4):717–729, April 2016.
- [51] K. Terzić, L. Hotz, and J. Šochman. Interpreting structures in man-made scenes: Combining low-level and high-level structure sources. In *International Conference on Agents and Artificial Intelligence*, Valencia, Spain, Jan 2010.
- [52] K. Terzić, S. Krishna, and J.M.H. du Buf. A parametric spectral model for texture-based salience. In *GCPR*, pages 331–342, Aachen, October 2015.
- [53] K. Terzić, D. Lobato, M. Saleiro, J. Martins, M. Farrajota, J.M.F. Rodrigues, and J.M.H. du Buf. Biological models for active vision: Towards a unified architecture. In *ICVS 2013, LNCS*, volume 7963, pages 113–122, Jul 2013.
- [54] K. Terzić, J.M.F. Rodrigues, and J.M.H. du Buf. Fast cortical keypoints for real-time object recognition. In *ICIP*, pages 3372–

- 3376, Melbourne, Sep 2013.
- [55] K. Terzić, J.M.F. Rodrigues, and J.M.H. du Buf. BIMP: A real-time biological model of multi-scale keypoint detection in V1. *Neurocomputing*, 150:227–237, 2015.
  - [56] Q. Wang, P. Yan, Y. Yuan, and X. Lia. Multi-spectral saliency detection. *Pattern Recognition Letters*, 34(1):34–41, January 2013.
  - [57] J. M. Wolfe and T. S. Horowitz. What attributes guide the deployment of visual attention and how do they do it? *Nature Reviews Neuroscience*, 5(6):495–501, 2004.
  - [58] J. Xie and Y. Fang. Dynamic texture recognition with video set based collaborative representation. *Image Vision Comput.*, 2016. In Press.
  - [59] Q. Yan, L. Xu, J. Shi, and J. Jia. Hierarchical saliency detection. In *CVPR*, 2013.

**Highlights**

- A novel texture model for visual salience is proposed
- A novel texture-based salience dataset is presented
- Combining texture features with colour and intensity improves performance